RAPID COMMUNICATION

Human Mutation

OFFICIAL JOURNAL
HGVS
HUMAN GENOME VARIATION SOCIETY
www.hgvs.org

Unexpected Allelic Heterogeneity and Spectrum of Mutations in Fowler Syndrome Revealed by Next-Generation Exome Sequencing

Emilie Lalonde,[1,3†] Steffen Albrecht,[2†] Kevin C.H. Ha,[1,3] Karine Jacob,[3] Nathalie Bolduc,[3] Constantin Polychronakos,[3,4] Pierre Dechelotte,[5] Jacek Majewski,[1,3] and Nada Jabado[3,4*]

[1]*McGill University and Genome Quebec Innovation Centre, Montreal, Canada;* [2]*Department of Pathology, Montreal Children's Hospital, McGill University Health Center, Montreal, Canada;* [3]*Departments of Human Genetics, McGill University Health Center, Montreal, Canada;* [4]*Departments of Pediatrics, Montreal Children's Hospital, McGill University Health Center, Montreal, Canada;* [5]*Department of Pathological Anatomy, CHU Clermont–Ferrand, Université d'Auvergne, France*

Communicated by Graham R. Taylor

Received 16 April 2010; accepted revised manuscript 14 May 2010.

Published online 1 June 2010 in Wiley InterScience (www.interscience.wiley.com). DOI 10.1002/humu.21293

ABSTRACT: Protein coding genes constitute approximately 1% of the human genome but harbor 85% of the mutations with large effects on disease-related traits. Therefore, efficient strategies for selectively sequencing complete coding regions (i.e., "whole exome") have the potential to contribute our understanding of human diseases. We used a method for whole-exome sequencing coupling Agilent whole-exome capture to the Illumina DNA-sequencing platform, and investigated two unrelated fetuses from nonconsanguineous families with Fowler Syndrome (FS), a stereotyped phenotype lethal disease. We report novel germline mutations in feline leukemia virus subgroup C cellular-receptor-family member 2, *FLVCR2*, which has recently been shown to cause FS. Using this technology, we identified three types of genetic abnormalities: point-mutations, insertions-deletions, and intronic splice-site changes (first pathogenic report using this technology), in the fetuses who both were compound heterozygotes for the disease. Although revealing a high level of allelic heterogeneity and mutational spectrum in FS, this study further illustrates the successful application of whole-exome sequencing to uncover genetic defects in rare Mendelian disorders. Of importance, we show that we can identify genes underlying rare, monogenic and recessive diseases using a limited number of patients ($n = 2$), in the absence of shared genetic heritage and in the presence of allelic heterogeneity.

Hum Mutat 31:918–923, 2010. © 2010 Wiley-Liss, Inc.

KEY WORDS: hydranencephaly–hydrocephaly; exome sequencing; deep sequencing; FLVCR2; Fowler syndrome

Introduction

Identification of rare monogenic diseases is of substantial interest to further our understanding of mechanisms of disease, biological pathways, and targeted therapies. To date, less than half of allelic variants responsible for monogenic disorders have been uncovered. This limited success is mainly due to the small numbers of available affected individuals for a given Mendelian disease (substantially reduced reproductive fitness leading to smaller pedigrees in affected families, etc.), or locus heterogeneity. All of these factors often lessen the power of traditional positional cloning strategies despite the advent of novel technologies, including single nucleotide polymorphism arrays (SNP microarrays). SNP arrays have been shown to help narrow areas of interest for further directed sequencing and are mainly powered (and thus limited) by families with shared genetic heritage (e.g., Mennonites, Amish, etc.) or with proven consanguinity [Laurier et al., 2006; Nishimura et al., 2005; Paisan-Ruiz et al., 2009; Strauss et al., 2005]. In contrast, deep resequencing of all human genes for discovery of allelic variants could potentially identify the gene underlying any given rare monogenic disease where a shared genetic heritage is not readily available [Shendure and Ji, 2008]. Massively parallel DNA sequencing technologies have rendered the whole-genome resequencing of individual humans increasingly practical, but cost remains a key consideration. An alternative approach involves the targeted resequencing of all protein-coding subsequences (that is, the exome), which requires $<2\%$ of the sequencing coverage required for the whole human genome [Choi et al., 2009; Ng et al., 2009] and has been very recently shown to be successful in identifying a Mendelian disorder [Ng et al., 2010].

The subject of our research, Fowler syndrome (FS), is a rare, prenatally lethal, disease that was first described in 1972 by Fowler et al. [1972]. There are less than 40 case reports [reviewed in Bessieres-Grattagliano et al., 2009; Williams et al., 2010], and all indicate a recurrent phenotype with hydrocephalus associated with progressive destruction of central nervous system tissue as a result of an unusual and characteristic proliferative vasculopathy. The occurrence of FS in consanguineous families and recurrence in both sexes is consistent with an autosomal recessive transmission. We investigated on the molecular level of two affected fetuses from two distinct French Canadian and French nonconsanguineous families. Using "next generation" exon sequencing (whole-exome sequencing coupling Agilent in-solution magnetic bead capture to the Illumina DNA sequencing platform), we identified

[†]The first two authors equally contributed to the manuscript.

*Correspondence to: Nada Jabado, Montreal Children's Hospital Research Institute, 4060 Ste. Catherine West, PT-239, Montreal, Qc, Canada H3Z 2Z3.
E-mail: nada.jabado@mcgill.ca

four separate germline alterations in the feline leukemia virus subgroup C cellular receptor family member 2 gene (*FLVCR2*, C14orf58 or FLJ20371 or MFSD7C; MIM♯ 610865) in the two patients who were compound heterozygotes for this disease. Mutations in *FLVCR2* have been very recently identified in FS [Meyer et al., 2010]. In three consanguineous families of Pakistani origin with FS, Meyer et al. [2010] performed a more traditional approach using autozygosity mapping (Affymetrix 250SNP arrays and microsatellite marker genotyping) in affected individuals. They demonstrated disease-linkage to chromosome 14q24.3, identified germline mutations in *FLVCR2* following direct sequencing of candidate genes within the target interval in the consanguineous cases, and further validated them in two additional patients with no documented consanguinity [Meyer et al., 2010]. Their approach illustrates a traditional gene mapping process, which even with the help of modern genotyping methods requires appropriate family structures and a sequential, usually lengthy process, involving identification of sizable candidate regions and systematic Sanger sequencing of a number of candidate genes. In our study, we use a much simpler and faster approach that makes full use of emerging technologies. We uncover two novel genetic alterations and a previously unsuspected high allelic heterogeneity in this very rare disorder. Importantly, we show that whole exome sequencing is a gene discovery approach that has major potential in identifying monogenic autosomal recessive disorders from a very small number affected individuals ($n = 2$) regardless of the need for shared genetic heritage status.

Materials and Methods

Patients Included in the Study

F1 was a female offspring of an unaffected nonconsanguineous French Canadian couple and was autopsied following pregnancy termination at the Montreal Children's Hospital. Pregnancy was terminated at 23 weeks' gestational age because of ventriculomegaly and limb deformities on fetal ultrasound examination. At autopsy, the fetus had features of fetal akinesia deformation sequence (arthrogryposis multiplex), with muscular atrophy, joint contractures, and cutaneous webbing. A 0.6-cm isolated atrial septal defect without other visceral malformations was also documented. Neuropathological findings showed bag-like cerebral hemispheres, with the cerebral mantle measuring only about 1–2 mm in thickness (Fig. 1A). No internal structures, such as basal ganglia or thalami, could be recognized (Fig. 1B). Brain stem and cerebellum were very small. Throughout the brain parenchyma, there were microcalcifications and hyperplastic microvessels forming glomeruloid structures (Fig. 1C). Some of the endothelial cells in the latter contained pale eosinophilic inclusions that stained strongly with PAS and were diastase resistant. Electron microscopy showed that these inclusions consisted of moderately electron-dense floculent material present in dilated rough endoplasmic reticulum (Fig. 1C). The residual brain parenchyma was highly disorganized. Spinal cord showed the same alterations and the eyes were normal. No vascular lesions were seen in any other organ. All of these abnormalities we report in F1 have been previously documented in the published FS cases [Al-Adnani et al., 2009; Castro-Gago et al., 2001; Fowler et al., 1972; Halder et al., 2003; Harper et al., 1983; Ibrahim et al., 2007; Usta et al., 2005; Witters et al., 2002]. Moreover, parents of F1 had lost a fetus with a phenotype of Fowler syndrome at 24 weeks of gestation 1 year prior to the termination of this pregnancy. Unfortunately, no frozen sample was available from the product of the first pregnancy and there were no other siblings in this family. DNA from F3, another fetus with FS sharing a similar phenotype (severely hypoplastic brain stem, cerebellum and spinal cord, and a glomeruloid vascular proliferation in all the brain including the cerebral cortex), was obtained through collaboration with a group in Clermont-Ferrand, France. This proband was from the kindred of family 4 described in Meyer et al. [2010]. All patient material was obtained following written consent from the families.

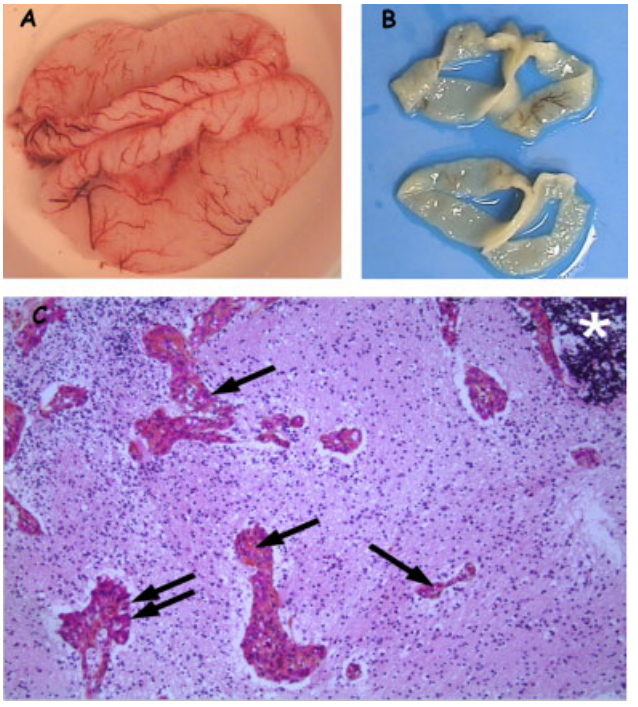

Figure 1. Neuropathological findings in case F1. **A:** Brain suspended in formalin solution. Notice the collapsed cerebral hemispheres. **B:** Coronal sections through the cerebral hemispheres. The cerebral mantle is extremely thin and there are no internal structures, such as basal ganglia and thalami. **C:** Histology. Medium power view shows hyperplastic microvessels (single arrows) and a glomeruloid structure (double arrow) along with an area of calcification (asterisk). (Hematoxylin-phloxine-saffron; original magnification 100 ×). [Color figure can be viewed in the online issue, which is available at www.interscience.wiley.com.]

Exome Capture, Sequencing, and Short-Read Alignment

A total of 3 μg of DNA was subject to the exome capture procedure using the SureSelect Human All Exon Kit (solution magnetic bead capture), according to manufacturer's protocols. The captured DNA was then sequenced using Illumina GAIIx sequencing. We used three lanes of single-end, 76 base pair reads per sample. Reads were first processed using ELAND2 to extract reads that passed quality control in FASTQ format. Next, the reads for each individual were aligned to the human genome (UCSC hg18, NCBI build 36.1) using BWA (version 0.5.7) due to its proven ability to identify insertions and deletions [Li and Durbin, 2009]. We found that BWA consistently had a higher or equal proportion of mapped reads across each chromosome compared to ELAND2. Parameters were adjusted to allow for identification of insertions and deletions longer than four base pairs. Reads mapping nonuniquely or to unfinished sequences (chrN_random

and chrN_hap) were filtered while all remaining reads were used for downstream variant detection.

Mapping Statistics

We obtained approximately 78.5 million reads for F1 and 62.7 million reads for F3 that passed quality control and could be mapped to the reference genome. The exome was defined in a similar manner as in Ng et al. [2009] based on the NCBI Consensus Coding Sequence (CCDS) database (version 20090327), which includes the protein coding regions of well-supported genes. Although this exome definition may miss some poorly supported genes or exons, it ensures that the regions included are truly protein coding. This is important because the majority of deleterious mutations are in coding regions. By conservatively limiting ourselves to entries with the "public" status and merging exons with overlapping coordinates to account for transcript isoforms, we generated a set of 161,778 nonoverlapping regions covering 27.5 Mb. In total, approximately 27.2 Mb of the exome was mappable by all of our reads. The BWA alignment provided an average of 23.2 million and 20.1 million uniquely mapping reads per lane for F1 and F3, respectively. In addition, 2.1 million reads in F1 and 1.7 million reads in F3 aligned to multiple positions in the genome. These repetitive locations likely represent gene families, such as paralogues and pseudogenes. The remaining 13.9 million reads in F1 and 17.3 million reads in F3 were unmappable. Approximately 50% of all the mappable reads were targeted to the exome, whereas 63% targeted to regions within 200 bp of the exons. The capture of intronic sequences directly flanking the exons allows for detection of intronic variants that may affect pre-mRNA splicing. Overall, using three lanes of sequencing per sample we obtained an average coverage of 66.8 × of the CCDS exome. This depth of coverage allows confident calling of both homozygous and heterozygous mutations.

Variant Identification

SNP and indel information was extracted from the alignment data using the Samtools package (version 0.1.7) [Li and Durbin, 2009; Li et al., 2009]. Thresholds of Phred-like SNP quality of 20 and 50 were used for SNPs and indels, respectively. Additional custom filtering criteria were then imposed on SNPs to minimize the false positive rates. Specifically, to identify a variant base the following conditions had to be satisfied: the minimum coverage threshold was set to four reads per base; at least 30% of covering reads had to support the alternate base; only reads with a minimum base quality of Phred-like score of 35 for the SNP position were considered; and, for SNPs with sufficient coverage, the alternate base had to be supported by reads originating from both DNA strands.

Variant Annotation

After removal of potential artifacts, the variants were functionally annotated using an in-house script, created by Louis Letourneau, and SIFT 4.0.3 [Kumar et al., 2009]. Additionally, SeattleSeq Annotation 5.00 was used to identify potential splice-site SNPs. Using these annotations, variants were filtered first for those that are novel (not present in dbSNP or the 1,000 Genomes databases) and then for those that are likely deleterious. We predicted that damaging SNPs would be either missense, nonsense, or splice-site SNPs whereas damaging indels would be in coding regions. The variants that met these criteria were used for downstream analysis.

Identification of FS-Causative Gene

To find the disease-associated gene, we systematically searched for genes in the following order: a gene with a single homozygous mutation seen in both F1 and F3; a gene with two distinct homozygous mutations in F1 and F3; and finally a gene for which F1 and F3 are compound heterozygotes. Only mutations passing all filters previously mentioned were considered in this pipeline. Mutation numbering is based on the NM_017791.2 cDNA sequence, with position +1 referring to the A of the ATG initiation codon, in accordance with the journal guidelines (www.hgvs.org/mutnomen). For protein nomenclature, codon 1 refers the initiation codon from the reference NP_060261.

Results and Discussion

Exome Sequencing Identifies FLVCR2 as Causal in FS

We sequenced exomes in a total of two unrelated fetuses with FS (F1 and F3) from two independent kindreds using Illumina Genome Analyzer IIx. An average of 5.3 Gb of mappable sequence was generated per affected individual as single-end, 76-bp reads. To distinguish potentially pathogenic mutations from other variants, we focused on nonsynonymous (NS) variants, splice acceptor, and donor site mutations (SS), and short coding insertions or deletions (indels; I), anticipating that synonymous variants would be far less likely to be pathogenic. We also presumed that the variants responsible for FS would be rare and therefore likely to be previously unidentified. A novel variant was defined as one that did not exist in the databases used for comparison, namely, dbSNP and 1000 Genomes.

As FS is a recessive disease, each proband was required to have two inactivated copies of the same gene; that is, both fetuses are either homozygotes or compound heterozygotes for a NS/SS/I mutation in the disease-causing gene. To identify the causative gene, we systematically searched for genes with a unique homozygous mutation in both samples, genes with distinct homozygous mutations in either sample, and genes for which both individuals are compound heterozygotes. Each fetus was found to have at least a single homozygous NS/SS/I variant in ~4,300 genes and at least a single heterozygous NS/SS/I variant in ~8,200 genes. Filtering these variants against the dbSNP and 1,000 Genomes databases reduced the candidate gene pool 100-fold for homozygous mutations and 10-fold for heterozygous mutations (Table 1).

Table 1. The Number of Genes Found in the Two Probands with Potentially Pathogenic Variants in Various Categories

	F1	F3
Homozygous		
NS/SS/I	4,275	4,408
Novel	59	81
Common to both samples	0	0
Different mutations in same gene	0	0
Heterozygous		
NS/SS/I	8,370	8,040
Novel	868	998
Compound heterozygotes	83	92
Common to both samples	1	1

Genes were screened for both homozygous and heterozygous variants. Each subsequent row introduces an additional filter on the variants within the two classes of variants. Novel variants refer to those not present in the dbSNP and 1,000 Genomes databases.

We first searched, unsuccessfully, for a homozygous mutation present in both probands. Similarly, no evidence was found for a single gene harboring different homozygous mutations in the two samples. We then proceeded to search for potentially damaging compound heterozygous variants. Individually, 83 and 92 candidate genes were identified in F1 and F3, respectively. Taking the intersection of these two lists revealed only one candidate gene, *FLVCR2*, which encodes the feline leukemia virus subgroup C cellular receptor family member 2 gene. Thus, comparison of exome data from two unrelated affected individuals was sufficient to identify *FLVCR2* as the sole candidate gene for FS. This finding is further corroborated by the recent publication by Meyer et al. [2010] at the time of finalizing our data.

The protein FLVCR2 has 12 transmembrane domains joined by extracellular loops (Fig. 2) and is predicted to belong to the major facilitator superfamily [Finn et al., 2010; Hunter et al., 2009], a class of small solute transporter proteins responsive to chemiosmotic ion gradients. Although we can identify the location of our variants with respect to FLVCR2's domains, further work is required to fully understand the exact consequences of these variants.

F1 is a compound heterozygote for two novel mutations. The first, c.997C>T, is in exon 4 (coordinates 75169725–75169792) and introduces an Alanine to Valine change, p.Ala326Val, at the end of the sixth transmembrane domain. The second one is in the 5′ splice site downstream of exon 7 (coordinates 75177051–75177156): c.1341+2T>C. It changes the GT donor site to GC and is the first pathogenic splice-site mutation found by exome sequencing. This mutation most likely leads to the skipping of exon 7 or retention of the intron following exon 7, disrupting the tenth transmembrane domain and potentially resulting in nonsense mediated decay, although the exact effects of this splice site substitution cannot be determined from this data. Neither mutation is annotated as a polymorphism in dbSNP nor 1,000 Genomes.

F3 is also a compound heterozygote. We identified the c.1192C>G (encoding p.Leu398Val) substitution in exon 6 and the c.329_334del6 deletion, p.Asn110_Phe112delinsIle, in exon 1 described previously by the group of Meyer et al. [2010]. This deletion results in a frameshift and in the shortening of the first extracellular loop in by three amino acids while the substitution is located two amino acids upstream of the ninth transmembrane domain. The *FLVCR2* genotype of this patient is identical to case 6 in family 4 of this report.

To determine whether the wild-type amino acids that are affected by the mutations are phylogenetically conserved, we used phastCons scores based on a Multiz alignment of 28 vertebrates, taken from the UCSC Genome Browser [Blanchette et al., 2004]. Scores range 0 to 1, where 1 is the most conserved. For F1, c.977C>T has a score of 0.997375 and c.1341+2T>C has a score of 0.976378. The scores of the F3 mutations are 1 and 0.992126 for c329_334del6 and c.1192C>G, respectively. Each mutation found affects at least one phylogenetically conserved residue, located either within a transmembrane domain or an extracellular loop. Altering these amino acids could result in structural changes within these important domains potentially leading to functional protein changes. Further functional studies are warranted and ongoing to test the impact of these mutations on protein function.

Validation of the Novel FLVCR2 Mutations Identified in F1

We had no DNA available from the parents of F1 to document that they were heterozygotes for the genetic changes seen in *FLVCR2*. However, we tested 95 DNA samples from unaffected

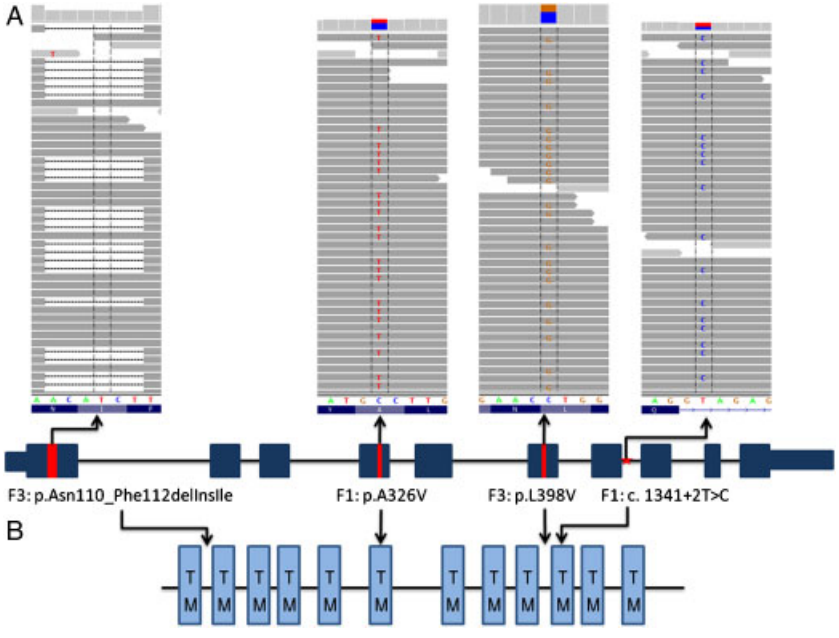

Figure 2. Schematic of the mutations found in F1 and F3 in both the gene and protein views. **A:** The four mutations in *FLVCR2* identified in F1 and F3 using whole exome sequencing as visualized using the Integrative Genomics Viewer from the Broad Institute (http://www.broadinstitute.org/igv). Mutations are also shown in their relative position along the gene (not to scale). **B:** Mutations in FLVCR2 are shown relative to the protein domains. Although the splice site mutation is not encoded, it likely results in retention of intron 7, disrupting the 10th transmembrane domain. (TM = transmembrane). Mutation numbering is based on the NM_017791.2 cDNA sequence, with position +1 referring to the A of the ATG initiation codon, in accordance with the journal guidelines (www.hgvs.org/mutnomen). For protein nomenclature, codon 1 refers the initiation codon from the reference NP_060261. [Color figure can be viewed in the online issue, which is available at www.interscience.wiley.com.]

individuals with similar geographic origin and did not identify the genetic changes seen in F1 on exons 1 and 4 of *FLVCR2*, further confirming that these are causative changes and not nonpathological variants. Along with the results of Meyer et al. [2010], these findings provide very strong evidence for the role of *FLVCR2* in FS, as well as the causative function the two new mutations identified by our group.

FLVCR2 Mutations and the Pathogenesis of FS

We identified four different mutations in a very rare monogenic disease: FS. In total, when combining our findings with those of Meyer et al. [2010], seven different mutations, including five missense variants, one nonsense mutation, and one deletion/insertion change, will have been found in *FLVCR2* and are potentially causative of FS. The features of FS have been reviewed in detail in two recent publications [Bessieres-Grattagliano et al., 2009; Williams et al., 2010]. Its pathological hallmark is the presence of hyperplastic microvessels forming glomeruloid structures throughout the central nervouse system (CNS). Some of these endothelial cells contain eosinophilic, PAS-positive, diastase-resistant inclusions that on electron microscopy are composed of moderately electron-dense floculent material present in dilated rough endoplasmic reticulum. The microvascular proliferation is associated with extensive necrosis and calcification of the CNS tissue. Destruction of brain tissue leads to hydranencephaly. The residual brain tissue is highly disorganized. The fetuses often but not invariably have features of fetal akinesia deformation sequence (arthrogryposis multiplex). There are no visceral malformations and the proliferative microangiopathy has not been described outside of the CNS. Importantly, it is unclear whether the microvascular proliferation is the result of the brain necrosis or its cause.

It is interesting to note that *FLVCR2* expression is not restricted to the CNS or to the vasculature (endothelium or pericytes). However, mutations in this gene induce a defect that is mainly, if not exclusively, restricted to the CNS and its vasculature, reenforcing the notion that brain angiogenesis is differentially regulated from angiogenesis in other body organs. FLVCR2 belongs to the major facilitator superfamily (MFS) of secondary carriers that transport small solutes in response to chemiosmotic ion gradients. It has been previously suggested that this transporter is specific for a calcium–chelate complex, and is involved in the regulation of growth and calcium metabolism, two processes involved in regulating angiogenesis, and the crosstalk between endothelial cells and pericytes. FLVCR1 (MIM♯ 609144), a paralog of FLVCR2 that shares 52% amino acid sequence identity, has been shown to be a human exporter of heme and to serve as a receptor for feline leukemia virus subgroup C (FeLV-C). FLVCR1 is critical for early erythropoiesis, and mutations in this receptor induce decreased to abrogated heme export, heme accumulation in erythroid progenitor, and their subsequent death [Keel et al., 2008]. *FLVCR1* null mice die in utero and have reduced myeloid and lymphoid cell growth and a disruption in early erythropoiesis with craniofacial and limb deformities [Keel et al., 2008]. A recent study shows that alternative splicing of *FLVCR1* transcripts lead to subsequent FLVCR1 insufficiency, and this in turn, acts as a contributing factor to the erythropoietic defect observed in Diamond-Blackfan anemia [Rey et al., 2008]. Wild-type FLVCR2 does not function as a receptor for FeLV-C or as a heme exporter; however, a single mutation of Asn463 to an acidic Asp residue in FLVCR2 extracellular domain 6 is sufficient to render it functional as an FeLV-C receptor [Brown et al., 2006]. This finding and data on FLVCR1 insufficiency secondary to a splicing defect in the gene reenforce our mutational findings as causative of abrogation/change of function in *FLVCR2*. If heme export is the major physiological function of FLVCR1, finding what FLVCR2 is exporting will prove crucial in understanding the pathogenesis of FS. Further studies are needed to determine what are the processes altered through *FLVCR2* mutations that are responsible of the exuberant vascular outgrowth and subsequent hydranencephaly.

We identify herein the gene responsible for a rare autosomal recessive disorder using direct whole exome resequencing on the smallest sample size reported for the identification of a monogenic disorder ($n = 2$). To date, there is only one other report that used this technology for the identification of a monogenic disorder. Ng et al. [2010] performed this type of methodology on four affected individuals including two siblings, and identified the gene responsible for Miller disease in addition to identifying mutations in *DNAH5* causing primary ciliary dyskineasia in the affected sibling pair. We were able, using this technology, to identify missense mutations, in-deletions, and intronic splice-site changes (first report using this technology to identify a pathogenic splice-site mutation), in only two individuals who were unrelated and who, in addition, came from kindred with no shared family heritage. Although we help uncover high allelic heterogeneity and mutation spectrum in a rare genetic disorder, FS, we show that this genetic approach is a much simpler and faster approach than traditional homozygosity mapping that makes full use of emerging technologies and is capable of identifying rare or common monogenic, recessive disorders. For dominant conditions, additional individuals are required, preferably from a single family whose family structure is known. By performing a linkage analysis prior to whole exome sequencing or resequencing, the region of interest could be narrowed to a reasonable size. Furthermore, this report emphasizes that it is now possible to directly identify a gene in a recessive Mendelian disorder using as few as two unrelated individuals and regardless of their kindred shared genetic heritage (consanguineous families and/or specific communities or genetic backgrounds) and in the presence of allelic heterogeneity.

Acknowledgments

The Cole Foundation (to N.J.). N.J. is the recipient of a Chercheur Boursier award from Fonds de Recherche en Sante du Quebec. J.M. is a recipient of a Canada Research Chair. We would like to thank Louis Letourneau for the use of his bioinformatics tools for filtering and annotations of SNPs. We would also like to thank the staff of the Genome Quebec sequencing platform, particularly Joana Dias, Alexandre Montpetit, and Pierre Lepage, with active participation and help in optimizing the techniques used in this project.

References

Al-Adnani M, Kiho L, Scheimberg I. 2009. Fowler syndrome presenting as a Dandy-Walker malformation: a second case report. Pediatr Dev Pathol 12:68–72.

Bessieres-Grattagliano B, Foliguet B, Devisme L, Loeuillet L, Marcorelles P, Bonniere M, Laquerriere A, Fallet-Bianco C, Martinovic J, Zrelli S, Leticee N, Cayol V, Etchevers HC, Vekemans M, Attie-Bitach T, Encha-Razavi F. 2009. Refining the clinicopathological pattern of cerebral proliferative glomeruloid vasculopathy (Fowler syndrome): report of 16 fetal cases. Eur J Med Genet 52:386–392.

Blanchette M, Kent WJ, Riemer C, Elnitski L, Smit AF, Roskin KM, Baertsch R, Rosenbloom K, Clawson H, Green ED, Haussler D, Miller W. 2004. Aligning multiple genomic sequences with the threaded blockset aligner. Genome Res 14:708–715.

Brown JK, Fung C, Tailor CS. 2006. Comprehensive mapping of receptor-functioning domains in feline leukemia virus subgroup C receptor FLVCR1. J Virol 80:1742–1751.

Castro-Gago M, Pintos-Martinez E, Forteza-Vila J, Iglesias-Diz M, Ucieda-Somoza R, Silva-Villar I, Codesido-Lopez J, Viso-Lorenzo A, Campos Y, Arenas J, Eirís-Puñal J. 2001. Congenital hydranencephalic–hydrocephalic syndrome with proliferative vasculopathy: a possible relation with mitochondrial dysfunction. J Child Neurol 16:858–862.

Choi M, Scholl UI, Ji W, Liu T, Tikhonova IR, Zumbo P, Nayir A, Bakkaloglu A, Ozen S, Sanjad S, Nelson-Williams C, Farhi A, Mane S, Lifton RP. 2009. Genetic diagnosis by whole exome capture and massively parallel DNA sequencing. Proc Natl Acad Sci USA 106:19096–19101.

Finn RD, Mistry J, Tate J, Coggill P, Heger A, Pollington JE, Gavin OL, Gunasekaran P, Ceric G, Forslund K, Holm L, Sonnhammer EL, Eddy SR, Bateman A. 2010. The Pfam protein families database. Nucleic Acids Res 38:D211–D222.

Fowler M, Dow R, White TA, Greer CH. 1972. Congenital hydrocephalus–hydrencephaly in five siblings, with autopsy studies: a new disease. Dev Med Child Neurol 14:173–188.

Halder A, Panigrahi I, Pal L. 2003. Fowler-like syndrome with extreme oligohydramnios, growth restriction and without muscular hypoplasia. Indian Pediatr 40:418–423.

Harper CG, Thomas W, ApSimon HT. 1983. Hydrocephalus and hypothalamic dysfunction in a young woman. Med J Aust 2:394–398.

Hunter S, Apweiler R, Attwood TK, Bairoch A, Bateman A, Binns D, Bork P, Das U, Daugherty L, Duquenne L, Finn RD, Gough J, Haft D, Hulo N, Kahn D, Kelly E, Laugraud A, Letunic I, Lonsdale D, Lopez R, Madera M, Maslen J, McAnulla C, McDowall J, Mistry J, Mitchell A, Mulder N, Natale D, Orengo C, Quinn AF, Selengut JD, Sigrist CJ, Thimma M, Thomas PD, Valentin F, Wilson D, Wu CH, Yeats C. 2009. InterPro: the integrative protein signature database. Nucleic Acids Res 37:D211–D215.

Ibrahim A, Murthy P, Arunkalaivanan AS. 2007. A case of recurrent first-trimester Fowler syndrome. J Obstet Gynaecol 27:201–202.

Keel SB, Doty RT, Yang Z, Quigley JG, Chen J, Knoblaugh S, Kingsley PD, De Domenico I, Vaughn MB, Kaplan J, Palis J, Abkowitz JL. 2008. A heme export protein is required for red blood cell differentiation and iron homeostasis. Science 319:825–828.

Kumar P, Henikoff S, Ng PC. 2009. Predicting the effects of coding non-synonymous variants on protein function using the SIFT algorithm. Nat Protoc 4:1073–1081.

Laurier V, Stoetzel C, Muller J, Thibault C, Corbani S, Jalkh N, Salem N, Chouery E, Poch O, Licaire S, Danse JM, Amati-Bonneau P, Bonneau D, Mégarbané A, Mandel JL, Dollfus H. 2006. Pitfalls of homozygosity mapping: an extended consanguineous Bardet-Biedl syndrome family with two mutant genes (BBS2, BBS10), three mutations, but no triallelism. Eur J Hum Genet 14:1195–1203.

Li H, Durbin R. 2009. Fast and accurate short read alignment with Burrows-Wheeler transform. Bioinformatics 25:1754–1760.

Li H, Handsaker B, Wysoker A, Fennell T, Ruan J, Homer N, Marth G, Abecasis G, Durbin R. 2009. The Sequence Alignment/Map format and SAMtools. Bioinformatics 25:2078–2079.

Meyer E, Ricketts C, Morgan NV, Morris MR, Pasha S, Tee LJ, Rahman F, Bazin A, Bessieres B, Dechelotte P, Yacoubi MT, Al-Adnani M, Marton T, Tannahill D, Trembath RC, Fallet-Bianco C, Cox P, Williams D, Maher ER. 2010. Mutations in FLVCR2 are associated with proliferative vasculopathy and hydranencephaly–hydrocephaly syndrome (Fowler syndrome). Am J Hum Genet 86:471–478.

Ng SB, Buckingham KJ, Lee C, Bigham AW, Tabor HK, Dent KM, Huff CD, Shannon PT, Jabs EW, Nickerson DA, Shendure J, Bamshad MJ. 2010. Exome sequencing identifies the cause of a mendelian disorder. Nat Genet 42:30–35.

Ng SB, Turner EH, Robertson PD, Flygare SD, Bigham AW, Lee C, Shaffer T, Wong M, Bhattacharjee A, Eichler EE, Bamshad M, Nickerson DA, Shendure J. 2009. Targeted capture and massively parallel sequencing of 12 human exomes. Nature 461:272–276.

Nishimura DY, Swiderski RE, Searby CC, Berg EM, Ferguson AL, Hennekam R, Merin S, Weleber RG, Biesecker LG, Stone EM, Sheffield VC. 2005. Comparative genomics and gene expression analysis identifies BBS9, a new Bardet-Biedl syndrome gene. Am J Hum Genet 77:1021–1033.

Paisan-Ruiz C, Scopes G, Lee P, Houlden H. 2009. Homozygosity mapping through whole genome analysis identifies a COL18A1 mutation in an Indian family presenting with an autosomal recessive neurological disorder. Am J Med Genet B Neuropsychiatr Genet 150B:993–997.

Rey MA, Duffy SP, Brown JK, Kennedy JA, Dick JE, Dror Y, Tailor CS. 2008. Enhanced alternative splicing of the FLVCR1 gene in Diamond Blackfan anemia disrupts FLVCR1 expression and function that are critical for erythropoiesis. Haematologica 93:1617–1626.

Shendure J, Ji H. 2008. Next-generation DNA sequencing. Nat Biotechnol 26:1135–1145.

Strauss KA, Puffenberger EG, Craig DW, Panganiban CB, Lee AM, Hu-Lince D, Stephan DA, Morton DH. 2005. Genome-wide SNP arrays as a diagnostic tool: clinical description, genetic mapping, and molecular characterization of Salla disease in an Old Order Mennonite population. Am J Med Genet A 138A:262–267.

Usta IM, AbuMusa AA, Khoury NG, Nassar AH. 2005. Early ultrasonographic changes in Fowler syndrome features and review of the literature. Prenat Diagn 25:1019–1023.

Williams D, Patel C, Fallet-Bianco C, Kalyanasundaram K, Yacoubi M, Dechelotte P, Scott R, Bazin A, Bessieres B, Marton T, Cox P. 2010. Fowler syndrome—a clinical, radiological, and pathological study of 14 cases. Am J Med Genet A 152A:153–160.

Witters I, Moerman P, Devriendt K, Braet P, Van Schoubroeck D, Van Assche FA, Fryns JP. 2002. Two siblings with early onset fetal akinesia deformation sequence and hydranencephaly: further evidence for autosomal recessive inheritance of hydranencephaly, fowler type. Am J Med Genet 108:41–44.